Numerical test of finite-size scaling predictions for the droplet condensation-evaporation transition

Andreas Nußbaumer[1], Johannes Zierenberg[2], Elmar Bittner[3] and Wolfhard Janke[2]

[1] Institut für Physik, Johannes Gutenberg Universität Mainz, Staudinger Weg 7, D-55128 Mainz, Germany

[2] Institut für Theoretische Physik, Universität Leipzig, Postfach 100 920, D-04009 Leipzig, Germany

[3] Institut für Theoretische Physik, Universität Heidelberg, Philosophenweg 16, D-69120 Heidelberg, Germany

E-mail: `wolfhard.janke@itp.uni-leipzig.de`

Abstract. We numerically study the finite-size droplet condensation-evaporation transition in two dimensions. We consider and compare two orthogonal approaches, namely at fixed temperature and at fixed density, making use of parallel multicanonical simulations. The equivalence between Ising model and lattice gas allows us to compare to analytical predictions. We recover the known background density (at fixed temperature) and transition temperature (at fixed density) in the thermodynamic limit and compare our finite-size deviations to the predicted leading-order finite-size corrections.

1. Introduction

Droplet formation is an essential process in nature with a variety of analogues in biological systems and material science. Of course, this generally involves non-equilibrium processes, e.g., the formation of nucleation prerequisites from local fluctuations while the surrounding gas acts as a density bath. Here, we consider instead a canonical setup in a finite system of size V with fixed temperature T and particle number N. If the gas is supersaturated, a variation of N or T results in the formation of equilibrium droplets [1, 2, 3, 4, 5]. In simple terms, the particle excess is subdivided to form a single macroscopic droplet in equilibrium with the surrounding vapor plus remaining excess. The resulting theory has been supported by numerous computational studies at fixed temperature, including the two-dimensional lattice gas [6, 7, 8] and three-dimensional Lennard-Jones gas [9, 10, 11]. The orthogonal approach at fixed density has received less attention [12], but recently enabled us to come closer to the asymptotic scaling regime for two- and three-dimensional lattice gas and three-dimensional Lennard-Jones gas [13]. In the following, we will compare the leading-order scaling corrections for a two-dimensional lattice gas at fixed temperature and fixed density from analytical predictions with numerical results.

2. Model

We consider a lattice gas in $d = 2$ dimensions. Excluded volume is modeled as lattice sites being either occupied by exactly one particle or empty, $n_i = \{0, 1\}$. Short-range interaction is included

by nearest-neighbor interaction ($\langle i, j \rangle$). The Hamiltonian is then

$$\mathcal{H} = -\sum_{\langle i,j \rangle} n_i n_j, \tag{1}$$

which is equivalent to an Ising model at fixed magnetization with $T^{\mathrm{Is}} = 4T$ and coupling constant $J = 1$ [14]. This originates in the identification of the spin state $s_i = 2n_i - 1$, which allows one to rewrite the Ising Hamiltonian

$$\mathcal{H}^{\mathrm{Is}} = -\sum_{\langle i,j \rangle} s_i s_j = 4\mathcal{H} - d(V - 4N), \tag{2}$$

considering that, on a simple hypercubic lattice, the sum over nearest neighbors yields d contributions and $N = \sum n_i$. The equivalence is then established by equating the Boltzmann factors $\exp(-\beta \mathcal{H})$, where $\beta = (k_{\mathrm{B}} T)^{-1}$. Evaluating $\beta^{\mathrm{Is}} \mathcal{H}^{\mathrm{Is}} = \beta \mathcal{H}$, where the constant shift is neglected due to physical unimportance, results in a simple rescaling of the temperature. When making use of the Ising equivalence all energy-related observables have to be rescaled correspondingly. The canonical Ising model is then equivalent to a grand-canonical lattice gas.

Exploiting the equivalence to the 2D Ising model, the critical point is located at $\beta_c = 4\beta_c^{\mathrm{Is}} = 2\ln\left(1 + \sqrt{2}\right) \approx 1.763$ or $k_{\mathrm{B}} T_c \approx 0.567$. For temperatures below this point, a spontaneous magnetization m_0 is observed and described by the Onsager-Yang solution [15, 16]:

$$m_0(\beta^{\mathrm{Is}}) = \left[1 - \sinh^{-4}(2\beta^{\mathrm{Is}})\right]^{1/8}. \tag{3}$$

This is directly related to the (grand-canonical) equilibrium background density $\rho_0 = (1 - m_0)/2$. The magnetic susceptibility is connected with the isothermal compressibility $\chi = \beta \kappa = \hat{\kappa}$ [8] and may be evaluated from sufficiently long series expansions (see, e.g., Ref. [17] and references therein), where

$$\chi(\beta^{\mathrm{Is}}) = \beta^{\mathrm{Is}} \sum_{i=0}^{n} c_i u^{2i} \quad \text{with} \quad u = \frac{1}{2 \sinh(2\beta^{\mathrm{Is}})}, \tag{4}$$

and $c = \{0, 0, 4, 16, 104, 416, 2224, 8896, 43840, 175296, 825648, 3300480, 15101920, ...\}$,[1] here considered up to the 300$^{\mathrm{th}}$ term. The equilibrium shape of a 2D Ising droplet is described by the Wulff plot (or shape), given by [18]

$$W = \frac{4}{(\beta^{\mathrm{Is}})^2} \int_0^{\beta^{\mathrm{Is}} \sigma_0} \mathrm{d}x \ \cosh^{-1}\left[\frac{\cosh^2(2\beta^{\mathrm{Is}})}{\sinh(2\beta^{\mathrm{Is}})} - \cosh(x)\right], \tag{5}$$

where $\sigma_0 = 2 + \ln[\tanh(\beta^{\mathrm{Is}})]/\beta^{\mathrm{Is}}$ and $\cosh^{-1}$ is referring to the inverse hyperbolic cosine. This will be relevant for the surface free energy of a (Wulff shaped) droplet of unit volume $\tau_{\mathrm{W}}^{\mathrm{Is}} = 2\sqrt{W}$. Being energy-related, the interface tension gets converted as $\tau_{\mathrm{W}} = \tau_{\mathrm{W}}^{\mathrm{Is}}/4$.

3. Method
In order to obtain numerical data at fixed temperature and at fixed density, we employed two different kinds of simulations. In both cases the underlying algorithm is the multicanonical method [19, 20, 21, 22]. The condensation transition is a first-order phase transition for which this method is well suited because it potentially allows one to overcome barriers in the free energy. The principle idea is to replace the Boltzmann weight $\exp(-\beta E)$ by an a priori unknown weight function $W(E)$, which is iteratively adapted in order to yield a flat histogram over a

---

[1] The coefficients were obtained from `http://www.ms.unimelb.edu.au/~iwan/ising/Ising_ser.html` [17].
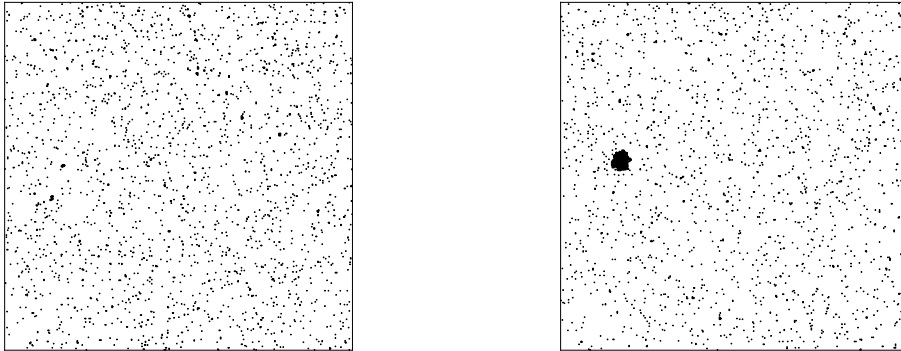
Figure 1. Snapshots of a two-dimensional lattice gas at fixed density above (left) and below (right) the condensation-evaporation temperature, showing a homogeneous gas phase and a droplet in equilibrium with surrounding vapor, respectively. Both plots show $N = 2500$ particles on a lattice of linear size $L = 500$, i.e., $\rho = 0.01$.

desired energy range. That way, energy states which are suppressed at a first-order phase transition are artificially enhanced and the simulation may transit back and forth between the involved coexisting phases. In the end, the simulation data has to be reweighted to estimates of expectation values at any temperature for which the probability distribution is covered by the flat histogram. The "optimal" weight function is reached if a simulation run produces a flat histogram, i.e., for a fixed c it holds $h(E_{\min})/h(E_{\max}) > c$. In part, we further make use of a parallel implementation [23, 24], which exploits the fact that in each iteration the histogram is an estimate of the probability distribution belonging to the current weight function. This allows one to distribute the sampling to independent Markov chains and to obtain a joint estimate as a simple sum of individual histograms. The procedure scales very well for the problem at hand [8].

The involved Monte Carlo updates include particle displacements to free nearest neighbors and random jumps to free sites. This corresponds to local and global Kawasaki updates. Errors are obtained using the Jackknife method [25] and standard error propagation. For further details of the employed methods we refer to Refs. [6, 7, 8, 13].

4. Theory of leading-order correction
A natural approach to particle condensation/evaporation is the consideration of a grand-canonical ensemble at fixed temperature, where the system relaxes to an equilibrium background contribution $N_0 = \rho_0 V$. Below the corresponding critical temperature the system is dominated either by particles (fluid branch) or by void space (gas branch) and $\rho_0 \neq 1/2$. Let us now consider the dilute gas branch well below the critical temperature and fix $N > N_0$. This results in the canonical ensemble of a supersaturated gas with particle excess $\delta N = N - N_0$. Initially, this excess goes into the gas phase while for sufficiently large excess droplet formation occurs.

In equilibrium droplet formation, the probability for intermediate-sized droplets was shown to vanish [3] and the scenario reduces to a homogeneous gas phase and an inhomogeneous phase of a droplet in equilibrium with surrounding vapor. This may be considered as the interplay of entropy maximization by fluctuations in the gas phase and energy minimization by forming a droplet [3, 4], see also Fig. 1. At fixed temperature it is possible to consider (fixed) thermal fluctuations and relate them to infinite-size temperature-dependent quantities, like the isothermal compressibility $\hat{\kappa}$ and the normalized surface free energy τ_{W}, see Sec. 2. The free energy may then be approximated by a contribution F_{fluc} from the fluctuation of

particle excess δN and a contribution F_{drop} from the single macroscopic droplet of size V_{D}:

$$F_{\mathrm{fluc}} = \frac{(\delta N)^2}{2\hat{\kappa}V} \qquad \text{and} \qquad F_{\mathrm{drop}} = \tau_{\mathrm{W}}(V_{\mathrm{D}})^{\frac{d-1}{d}}. \qquad (6)$$

These contributions are idealized with possible sources of corrections in both the Gaussian approximation and the droplet shape for finite systems.

In the two-phase scenario, the particle excess may be decomposed into the excess inside the droplet δN_{D} and the excess in the fluctuating phase δN_{F}, i.e., $\delta N = N - N_0 = \delta N_{\mathrm{D}} + \delta N_{\mathrm{F}}$. Linking the droplet size to the particle excess inside the droplet, one expects $\delta N_{\mathrm{D}} = (\rho_{\mathrm{L}} - \rho_0)V_{\mathrm{D}}$, where ρ_{L} and ρ_0 are the background liquid and gas density, respectively. Then, one may introduce a scalar fraction

$$\lambda = \delta N_{\mathrm{D}}/\delta N, \qquad (7)$$

such that $\delta N_{\mathrm{D}} = \lambda \delta N$ and $\delta N_{\mathrm{F}} = (1-\lambda)\delta N$. The total free energy $F = F_{\mathrm{drop}} + F_{\mathrm{fluc}}$ becomes

$$F = \tau_{\mathrm{W}}\left(\frac{\lambda \delta N}{\rho_{\mathrm{L}} - \rho_0}\right)^{\frac{d-1}{d}} + \frac{(1-\lambda)^2(\delta N)^2}{2\hat{\kappa}V} = \tau_W \left(\frac{\delta N}{\rho_{\mathrm{L}} - \rho_0}\right)^{\frac{d-1}{d}}\left(\lambda^{\frac{d-1}{d}} + \Delta(1-\lambda)^2\right), \quad (8)$$

with a dimensionless "density" parameter

$$\Delta = \frac{(\rho_{\mathrm{L}} - \rho_0)^{\frac{d-1}{d}}}{2\hat{\kappa}\tau_W} \frac{(\delta N)^{\frac{d+1}{d}}}{V} = \frac{(\rho_{\mathrm{L}} - \rho_0)^{\frac{d-1}{d}}}{2\hat{\kappa}\tau_{\mathrm{W}}}(\rho - \rho_0)^{\frac{d+1}{d}}\ V^{\frac{1}{d}}. \qquad (9)$$

At fixed temperature $\rho_{\mathrm{L}}, \rho_0, \hat{\kappa}, \tau_W$ are constants and Δ may be interpreted as an unusual density. In principle, all constants may be estimated and for the present case, equivalent to the 2D Ising model, the parameters are even known exactly or with very high precision.

This leading-order formulation allows one to obtain the fraction of particles inside the largest droplet λ as a function of Δ in the limit of large systems, by minimizing Eq. (8) with respect to λ. It turns out (for details see Refs. [3, 4]) that there exists a constant Δ_{c} below which no droplet forms ($\lambda = 0$) and above which a single macroscopic droplet exists with non-trivial $\lambda > \lambda_{\mathrm{c}}$:

$$\Delta_{\mathrm{c}} = \frac{1}{d}\left(\frac{d+1}{2}\right)^{\frac{d+1}{d}} \overset{\mathrm{2D}}{=} 0.9186... \qquad \text{and} \qquad \lambda_{\mathrm{c}} = \frac{2}{d+1} \overset{\mathrm{2D}}{=} 2/3. \qquad (10)$$

The result $\lambda(\Delta)$ describes the expectation value of the equilibrium droplet size in the limit of large systems without any free parameter. As mentioned before, this already includes the leading-order finite-size corrections for idealized assumptions. In fact, Eq. (9) may be rewritten at each finite-size transition density ρ_{c}, where $\Delta(\rho_{\mathrm{c}}) = \Delta_{\mathrm{c}}$. For a lattice gas model with particle-hole symmetry, $\rho_{\mathrm{L}} = 1 - \rho_0$, this yields to leading order

$$\rho_{\mathrm{c}} = \rho_0 + \left(\frac{2\hat{\kappa}\tau_{\mathrm{W}}\Delta_{\mathrm{c}}}{(1-2\rho_0)^{\frac{d-1}{d}}}\right)^{\frac{d}{d+1}} V^{-\frac{1}{d+1}}, \qquad \text{or} \qquad m_{\mathrm{c}} = m_0 - 2m_0\left(\frac{\chi\tau_{\mathrm{W}}^{\mathrm{Is}}\Delta_{\mathrm{c}}}{2m_0^2}\right)^{\frac{d}{d+1}} V^{-\frac{1}{d+1}}, \ (11)$$

where the second formulation is in terms of the Ising model at fixed magnetization. This is the notation of Biskup et al. [3, 4], but is in quantitative agreement with the (independent) result of Neuhaus and Hager [2]. For the 2D Ising model, they find the same leading scaling behavior $\Delta m(L) = A_{\mathrm{cond}}L^{-2/3}$, with the amplitude $A_{\mathrm{cond}} = 0.23697...$ for $\beta^{\mathrm{Is}} = 0.7$ and Eq. (11) yields $A = 0.236965...$ for the corresponding constants.[2]

---

[2] For $\beta^{\mathrm{Is}} = 0.7$ we obtain $m_0 \simeq 0.99016$, $\chi \simeq 0.019310$ and $\tau_{\mathrm{W}}^{\mathrm{Is}} \simeq 4.5758$.
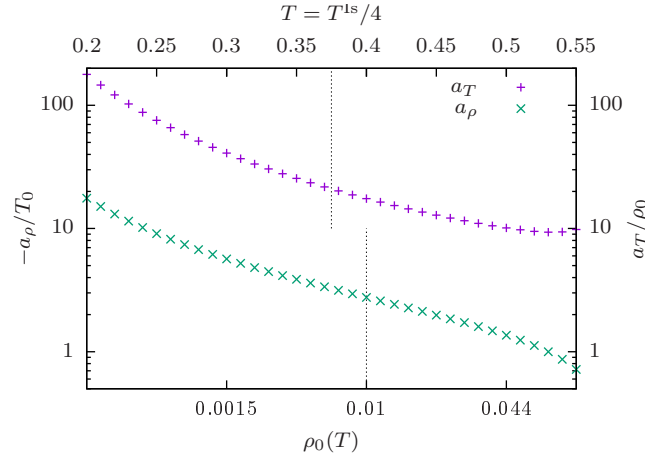
Figure 2. Leading-order normalized finite-size correction amplitude at fixed temperature T and fixed density ρ. The densities $\rho_0(T)$ on the lower x-axis are calculated from the Onsager-Yang solution Eq. (3). The data points are obtained by numerically evaluating Eq. (14) and Eq. (15). Dashed lines indicate the parameters considered below.

In the following, we will numerically review the leading-order finite-size scaling predictions. We consider directly the scaling of the factual transition density (or magnetization) at fixed temperature [6, 7] and compare to the scaling of the transition temperature at fixed density [13]. Albeit the possibility of logarithmic corrections, we consider empirical higher-order corrections as powers of the leading term if necessary. Our fit ansatz for the leading-order correction is

$$\rho_c = \rho_0 + a_T V^{-1/3} + \mathcal{O}\left(V^{-2/3}\right) \qquad\qquad \text{at fixed } T, \qquad (12)$$

$$T_c = T_0 + a_\rho V^{-1/3} + \mathcal{O}\left(V^{-2/3}\right) \qquad\qquad \text{at fixed } \rho. \qquad (13)$$

By comparing to Eq. (11), a_T can be related to Δ_c. Similarly, a relation for a_ρ follows from a Taylor expansion around T_0 of a reformulated Eq. (9), namely $\Delta^{2/3} V^{-1/3} = f(\rho, T)$. From the equivalence to the Ising model, we identify $f(\rho, T)$ with $f(m, T^{\mathrm{Is}}) = (m_0(T^{\mathrm{Is}}) - m)[m_0(T^{\mathrm{Is}})/2]^{1/3}[\chi(T^{\mathrm{Is}})\tau_{\mathrm{W}}^{\mathrm{Is}}(T^{\mathrm{Is}})]^{-2/3}$ (see Ref. [13] for details), which leads to

$$\Delta_c = a_T^{3/2} 2 m_0^{1/2} / \chi \tau_{\mathrm{W}}^{\mathrm{Is}} \qquad\qquad \text{at fixed } T, \qquad (14)$$

$$\Delta_c = \left[a_\rho 4 f'(m, T_0^{\mathrm{Is}})\right]^{3/2} \qquad\qquad \text{at fixed } \rho. \qquad (15)$$

This may be evaluated numerically considering Eqs. (3)–(5) and (10) to yield estimates of the leading-order correction. Figure 2 shows results for a range of temperatures and according densities, related by the Onsager-Yang solution Eq. (3). The relative leading-order corrections at fixed temperature are almost an order of magnitude larger than at fixed density. However, in the practical finite-size scaling analysis higher-order corrections are of more significance, which cannot be estimated by the current theory.

5. Results
We will start the discussion with our findings at fixed temperature $k_{\mathrm{B}}T = 0.375$. Most results are analyses of Monte Carlo time series data obtained by refined methods analogous to Refs. [6, 7]. For each system size, we set up individual simulations at selected densities around the expected transition region, see Fig. 3 (left). For densities below the finite-size transition point $\Delta < \Delta_c$
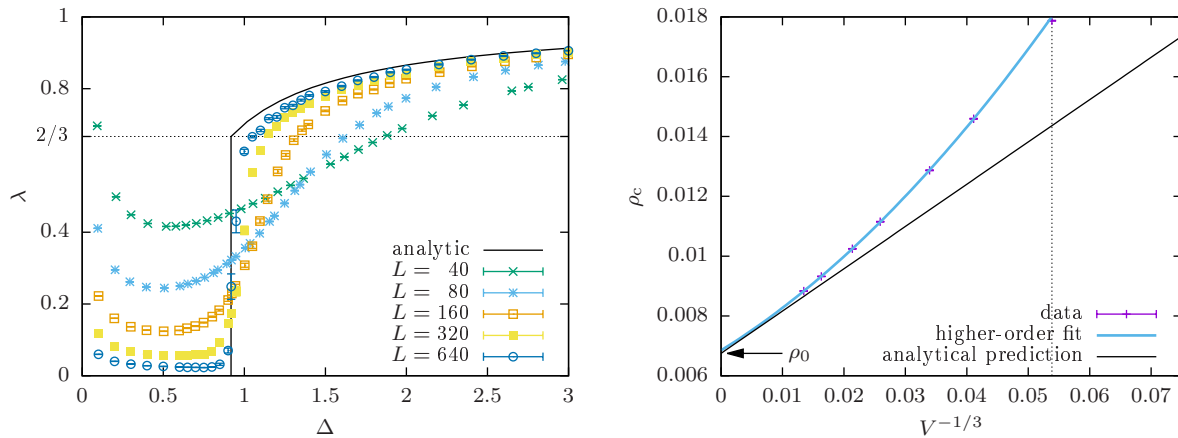
Figure 3. Droplet formation at fixed temperature $k_BT = 0.375$ [6, 7]. (left) Fraction of excess versus rescaled dimensionless density Δ. (right) Finite-size scaling of the transition density ρ_c. The black line shows the predicted leading-order scaling and the blue line is a higher-order fit to the data. ρ_0 is the analytically known thermodynamic limit. The dotted vertical line indicates the end of the fitting range ($L = 80$).

the system is in the gaseous phase and for $\Delta > \Delta_c$ a single macroscopic droplet forms in accordance with theory. In fact, the results are obtained in the equivalent formulation of an Ising model at fixed magnetization, but here discussed in the generic formulation of a lattice gas. In order to ensure ergodic sampling, we augmented the Kawasaki Monte Carlo update with a multicanonical scheme to locally sample a flat histogram including transition states and ensuring a good sampling of the energy probability distribution up to suppressions of 30 orders of magnitude. The fraction of excess in the largest droplet, Eq. (7), is obtained by a two-step process. Firstly, all clusters in the system are determined, where we define a cluster as alike sites connected via the nearest-neighbor property. The largest cluster is the background (or gaseous phase), while the second largest cluster forms the droplet we are interested in. Then, the volume of the droplet is identified as all sites confined by the boundary, including the enclosed holes. The fraction λ is then the ratio of the droplet volume and the expected equilibrium volume of full excess $V_\delta = (N - \rho_0 L^2)/(1 - 2\rho_0)$. The result of this procedure is shown in Fig. 3 (left). We also show the limiting case that can be found as the solution of Eq. (8) as solid black line. Every data point is the average of 10^6 Monte Carlo sweeps (L^2 updates). At the infinite-size transition density, the analytical prediction is $\lambda_c = 2/3$, see Eq. (10). Hence, we estimate the finite-size transition point as the density ρ_c for which $\lambda(\rho_c, L) = 2/3$. Technically, we do a linear interpolation of the data points in Fig. 3 (left) and search for the intersection.

The resulting scaling of the transition density is shown in Fig. 3 (right) in dependence on $V^{-1/3}$ as expected from Eq. (12). The thermodynamic limit is given by the Onsager-Yang solution, $\rho_0 \simeq 0.00675$. From the analytical prediction in Eq. (14), we expect for the leading-order correction at fixed temperature $k_BT = 0.375$ that $\Delta_c \simeq 0.919 \approx (6.6833 \, a_T)^{3/2}$ and thus $a_T \approx 0.141$,[3] shown in the figure as a black line. The data does not allow for a qualitatively satisfying leading-order fit, but the largest system size is already close to the predicted finite-size deviation. Considering the next higher empirical correction, i.e., $\rho_c = \rho_0 + a_T V^{-1/3} + b_T V^{-2/3}$, allows for a decent fit which yields for $L > 80$ the result $\rho_0 = 0.00676(5)$ and $a_T = 0.135(3)$ with goodness-of-fit parameter $Q \approx 0.02$. The estimated limit is in good agreement with the

---

[3] For $k_BT = k_BT^{Is}/4 = 0.375$ we obtain $m_0 \simeq 0.9865$ or $\rho_0 \simeq 0.00675$, $\chi = \hat{\kappa} \simeq 0.02708$, and $\tau_W^{Is} \simeq 4.2454$ or $\tau_W \simeq 1.0613$.
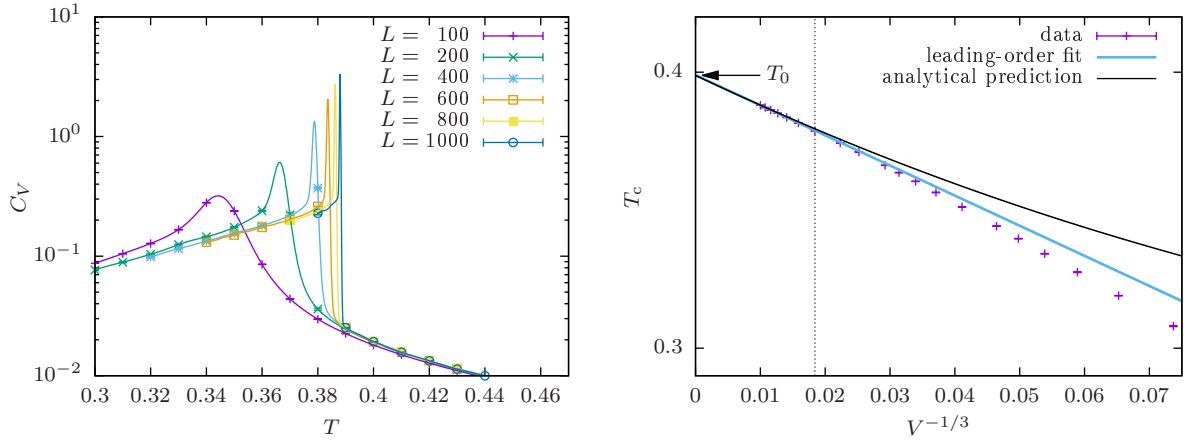
Figure 4. Droplet formation at fixed density $\rho = 10^{-2}$ [13]. (left) Specific heat with exemplary data points that indicate the size of the error. (right) Finite-size scaling of the transition temperature. The black line shows the numerical evaluation of Eq. (9) at fixed ρ and the blue line is a leading-order fit. T_0 is the analytically known thermodynamic limit. The dotted vertical line indicates the end of the fitting range ($L = 400$).

analytical prediction ρ_0 marked by the arrow. Using Eq. (15) with error propagation yields the estimate $\Delta_c = 0.86(3)$, which is below but consistent with the theoretical prediction. We notice that the choice of the intersection in $[0, 2/3]$ strongly influences the size of the higher-order corrections.

We next turn to the orthogonal setup of a fixed density $\rho = 10^{-2}$ with varying temperature [13]. Here, the multicanonical method is more straightforward and for each system size we may perform a single (yet parallel) simulation with up to 128 cores and 1.28×10^6 measurements in the final production run. This yields a full temperature range of expectation values and the transition temperature may be determined precisely as the peak of the specific heat $C_V = k_{\mathrm{B}} \beta^2 \left(\langle E^2 \rangle - \langle E \rangle^2 \right) / N$, see Fig. 4 (left). For details see Ref. [13], from which we recapture the data in order to compare to the leading-order results at fixed temperature. For $\rho = 10^{-2}$, the numerical evaluation of the Onsager-Yang solution Eq. (3) yields $T_0 \simeq 0.39882$, which is the expected thermodynamic limit. From the analytical prediction Eq. (15), we expect for the leading-order correction that $\Delta_c \simeq 0.919 \approx (-0.85177\, a_\rho)^{3/2}$ and thus $a_\rho \approx -1.109$.

Figure 4 (right) shows the finite-size transition temperature as a function of the expected leading-order scaling correction. In two dimensions, we can numerically evaluate Eq. (9) at fixed density for various system sizes. This gives the (analytical) leading-order finite-size estimate of the transition temperature, shown as a black line. We can see that this predicted leading-order behavior is only approximately reached for very large system sizes of about $L \simeq 500$. For small system sizes, the leading-order solution strongly deviates, which may be expected from the simplified assumptions. A leading-order fit for $L \geq 400$ yields $T_0 = 0.39891(5)$ and $a_\rho = -1.091(4)$ with $Q \approx 0.25$. The limit is in good agreement with the analytical value. Using Eq. (15) with error propagation yields the estimate $\Delta_c = 0.896(5)$. This is close to, but differs slightly from, the predicted value. As for the case of fixed temperature, this is below the theoretical prediction. The fit error is too small in order to be fully consistent, which may be accounted to missing higher-order corrections. We also tried the empirical higher-order corrections, however, it did not improve our estimates. This may be explained by additional corrections, e.g., logarithmic ones, which were not considered. Still, the qualitatively good leading order fit shows that in this setup we are close to the asymptotic scaling regime.

6. Conclusions

We numerically investigated the leading-order finite-size scaling corrections of the two-dimensional droplet condensation-evaporation transition at fixed temperature and density, respectively. In both cases we could recover the analytically known thermodynamic limits, in part by considering empirical higher-order corrections. The leading-order corrections were found to be slightly smaller than but consistent with the analytical predictions [3, 4]. This shows that the established theory is able to qualitatively describe the finite-size deviations; in case of the two-dimensional lattice gas already for system sizes $L \simeq 500$.

Acknowledgments

References

[1] Binder K and Kalos M H 1980 *J. Stat. Phys.* **22** 363
[2] Neuhaus T and Hager J 2003 *J. Stat. Phys.* **113** 47
[3] Biskup M, Chayes L and Kotecký R 2002 *Europhys. Lett.* **60** 32
[4] Biskup M, Chayes L and Kotecký R 2003 *J. Stat. Phys.* **116** 175
[5] Binder K 2003 *Physica A* **319** 99
[6] Nußbaumer A, Bittner E, Neuhaus T and Janke W 2006 *Europhys. Lett.* **75** 716
[7] Nußbaumer A, Bittner E and Janke W 2008 *Phys. Rev. E* **77** 041109
[8] Zierenberg J, Wiedenmann M and Janke W 2014 *J. Phys: Conf. Ser.* **510** 012017
[9] MacDowell L G, Virnau P, Müller M and Binder K 2004 *J. Chem. Phys.* **120** 5293
[10] MacDowell L G, Shen V K and Errington J R 2006 *J. Chem. Phys.* **125** 034705
[11] Schrader M, Virnau P and Binder K 2009 *Phys. Rev. E* **79** 061104
[12] Martinos S, Malakis A and Hadjiagapiou I 2007 *Physica A* **384** 368
[13] Zierenberg J and Janke W 2015 *Phys. Rev. E* **92** 012134
[14] Lee T D and Yang C N 1952 *Phys. Rev.* **87** 410
[15] Onsager L 1949 *Nuovo Cimento (Suppl.)* **6** 261
[16] Yang C N 1952 *Phys. Rev.* **85** 808
[17] Boukraa S, Guttmann A J, Hassani S, Jensen I, Maillard J M, Nickel B and Zenine N 2008 *J. Phys. A: Math. Theor.* **41** 455202
[18] Leung K and Zia R K P 1990 *J. Phys. A: Math. Gen.* **23** 4593
[19] Berg B A and Neuhaus T 1991 *Phys. Lett. B* **267** 249
[20] Berg B A and Neuhaus T 1992 *Phys. Rev. Lett.* **68** 9
[21] Janke W 1992 *Int. J. Mod. Phys. C* **3** 1137
[22] Janke W 1998 *Physica A* **254** 164
[23] Zierenberg J, Marenz M and Janke W 2013 *Comput. Phys. Commun.* **184** 1155
[24] Zierenberg J, Marenz M and Janke W 2014 *Physics Procedia* **53** 55
[25] Efron B 1982 *The Jackknife, the Bootstrap and Other Resampling Plans* (Society for Industrial and Applied Mathematics)